Conformal Mapping and Applications to Ideal Fluid Flow

Elizabeth Cutting[1], Madison Jones[1], and Matt Harper[1]

[1]Undergraduate Department of Applied Mathematics, University of Colorado, Boulder

29 April 2024

Abstract

A *conformal map* is a transformation which preserves local angles. An analytic function $f : S \to \mathbb{C}$, where S is an open subset of the complex plane, is *conformal* at any point where $f'(z) \neq 0$. Such transformations are especially useful for their ability to simplify problems satisfying Laplace's equation, such as heat conduction, electrostatics, and ideal fluid flow. This paper introduces the derivation and properties of conformal maps and further investigates applications to ideal fluid flow, including the Joukowski transform for airfoil analysis.

Introduction

This paper will begin by introducing the idea of a conformal map. A *conformal map* is a transformation that preserves local angles. We prove that a function can be verified as a conformal map if it satisfies two main requirements by exploring a geometric proof. The function must be analytic and must have a nonzero derivative to be conformal at a given point. We then explore more examples and transformations, noting how the properties of various functions align with the requirements for conformality.

The main benefit of conformal mapping is that we are able to transform into a simpler domain. Due to their analyticity, conformal mappings satisfy the Cauchy-Riemann equations, and therefore the real and imaginary parts satisfy Laplace's Equation. We then demonstrate a theorem to understand how conformal maps transform solutions to Laplace's equation, and equipped with this, we explore ideal fluid flow. We note how conformal mappings allow us to solve simple problems with uniform flow and then transform our result back into the original domain.

Finally, specific analysis is conducted on a particular application to airfoils: the Joukowski transform. Under the assumptions of ideal fluid flow we study the transformation of various circles. Finally, we conclude by studying the streamlines at varying angles on a given airfoil.

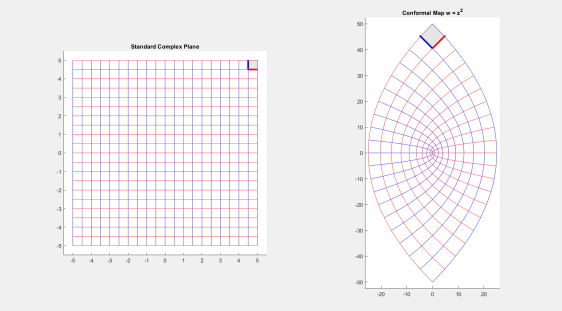

Figure 1: $w = z^2$

Project Description

Conformal Mapping

Using the definition of conformal mapping from the introduction, consider one of the most famous and simple examples of conformal mapping: $f(z) = z^2$. We can plot view this mapping through the lens of grid lines that make up the complex plane. Figure 1 was produced by letting $z = x + iy$ and drawing out the real and imaginary parts. Then, the function was applied to each line and individually plotted. All conformal mapping figures throughout the paper were constructed in the same way using MATLAB. Much of this code was modelled after MathWorks Documentation. [1]

Figure 1 is best observed by noting the transformation of each individual line. First, let us consider the imaginary axis. When a value iy is squared, we note that $(i)^2 = -i \implies (iy)^2 = -y^2$ which becomes a purely real value. If we now consider the purely real values ($z = x$), when we take x^2 we note that the resulting value remains a purely real value. These two concepts are demonstrated in the visual and therefore allows us to recognize that the function conforms to intuition.

We also note that at each individual local point, all of the angles of the original function are preserved. In this case, all of the intersections between horizontal and vertical lines in the standard complex plane are orthogonal which is identical in the transformed plane even though the lines curve. However, we note that this property is not present as we approach the origin, appearing as though it is not conformal here. We will explore the reasoning for this.

When beginning to analyze conformal mappings, it is often difficult, if not impossible, to check every individual point and angle to confirm the two properties hold true. Therefore, a theorem regarding the verification of a function as a conformal mapping can be verified and applied.

Theorem 1. *If $f(z)$ is an analytic function and $f'(z) \neq 0$, then f defines a conformal mapping in the complex plane.*

Proof.
Let f be an analytic function in some domain $\mathcal{D} \subseteq \mathbb{C}$.
Let $z = x + iy$, such that $f(x, y) = u(x, y) + iv(x, y)$ where u and v satisfy the Cauchy Riemann equations.

Define the Jacobian of f as J:

$$\begin{aligned} J(x,y) &= \begin{bmatrix} u_x(x,y) & u_y(x,y) \\ v_x(x.y) & v_y(x,y) \end{bmatrix} \\ &= \begin{bmatrix} u_x(x,y) & u_y(x,y) \\ -u_y(x.y) & u_x(x,y) \end{bmatrix} \text{ by Cauchy-Riemann} \\ &\text{Let } u_x = r\cos\theta \text{ and } u_y = r\sin\theta \\ &= r\begin{bmatrix} \cos\theta & \sin\theta \\ -\sin\theta & \cos\theta \end{bmatrix} \end{aligned}$$

Consider two smooth curves c_1 and c_2, parameterized as $c_1(t) = (u_1(t), v_1(t))$ and $c_2(t) = (u_2(t), v_2(t))$.
Let $c_1(0) = c_2(0) = z_0$.
Then,

$$\begin{aligned} f(c_1(t))'(0) &= \frac{\partial(u,v)}{\partial(x,y)} \cdot c_1(0) \cdot \frac{dc_1}{dt}(0) \\ &= J(x,y)\begin{bmatrix} \frac{du_1}{dt} \\ \frac{dv_1}{dt} \end{bmatrix} \end{aligned}$$

Likewise,

$$f(c_2(t))'(0) = J(x,y)\begin{bmatrix} \frac{du_2}{dt} \\ \frac{dv_2}{dt} \end{bmatrix}$$

We will consider the case where $f'(z) \neq 0$.
Further, note that f consists of a transformation of an orthogonal matrix since

$$\begin{bmatrix} \cos\theta & \sin\theta \\ -\sin\theta & \cos\theta \end{bmatrix} \cdot \begin{bmatrix} \cos\theta & -\sin\theta \\ \sin\theta & \cos\theta \end{bmatrix} = \begin{bmatrix} 1 & 0 \\ 0 & 1 \end{bmatrix}$$

and f scales by a factor of r. This transformation implies that the angle between tangent vectors is preserved.
Finally, note that the orientation of the curve is preserved since the determinant of $\frac{J(x,y)}{r}$ is 1:

$$\det(\tfrac{J}{r}) = \det\begin{bmatrix} \cos\theta & \sin\theta \\ -\sin\theta & \cos\theta \end{bmatrix} = \cos^2\theta + \sin^2\theta = 1$$

By the properties of orthogonal matrices, the angles of the function must be preserved along with the orientation.
Therefore, we conclude f is a conformal mapping where $f'(z) \neq 0$. □

Let this theorem be applied to our first example, where $f(z) = z^2$.

$$\begin{gathered} f(z) = z^2 \implies f'(z) = 2z. \\ f'(z) = 2z = 0 \implies z = 0 \\ f'(z) \neq 0 \text{ for } z \neq 0. \end{gathered}$$

Therefore, at all points $z \in \mathbb{C}$ for $z \neq 0$, $f(z)$ defines a conformal map.

Consider another example, $g(z) = e^z$.

$$g(z) = e^z \implies g'(z) = e^z$$
$$g'(z) = e^z \neq 0 \text{ for all } z \in \mathbb{C}$$

Therefore, $g(z)$ is a conformal map everywhere which is visualized below.

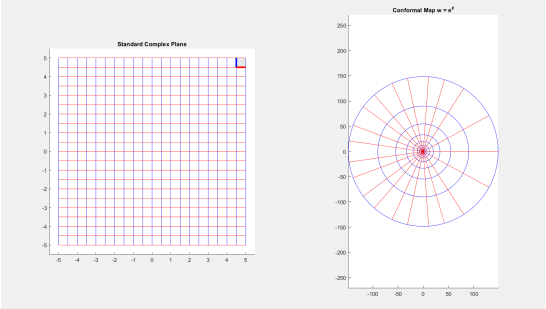

We can further interpret this result in terms its real and imaginary components. By letting $z = x + iy$, $g(x + iy) = e^{x+iy} = e^x e^{iy} = e^x(\cos y + i \sin y)$ by Euler's Formula. Therefore the real part, x, will determine the magnitude of the result and the imaginary part will determine the angle which is reflected in the radial circles corresponding to the imaginary lines.

In contrast, let us now consider the example $h(z) = e^{iz}$. $h(z)$ has a similar structure to e^z but with a key difference. Note $e^{iz} = e^{i(x+iy)} = e^{-y}e^{ix}$. Therefore, the real parts correspond to the argument and the imaginary parts correspond to the magnitude.

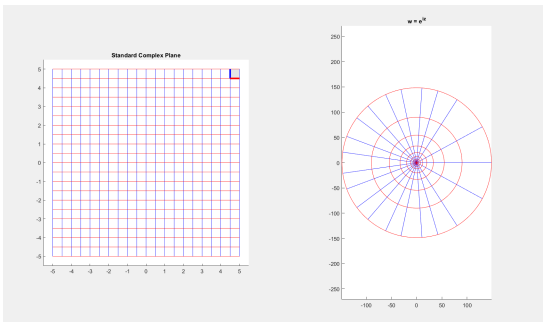

We can also verify that h defines a conformal map:

$$h(z) = e^{iz} \implies h'(z) = ie^{iz}$$
$$h'(z) = ie^{iz} \neq 0 \text{ for all } z \in \mathbb{C}$$

Therefore, as above, we can conclude that $h(z) = e^{iz}$ defines a conformal map for all $z \in \mathbb{C}$.

Beyond these seemingly elementary examples, we will now consider the class of conformal mapping known as the Möbius transform. This transform takes the form:

$$f(z) = \frac{az + b}{cz + d}, \ ad \neq bc \tag{1}$$

We note this is a ratio of entire functions (meromorphic) and the only singular point occurs at $z = -\frac{d}{c}$. As such, $f(z)$ is analytic for $z \in \mathbb{C}/\{-\frac{d}{c}\}$ [2]. We can also verify the conformality of this

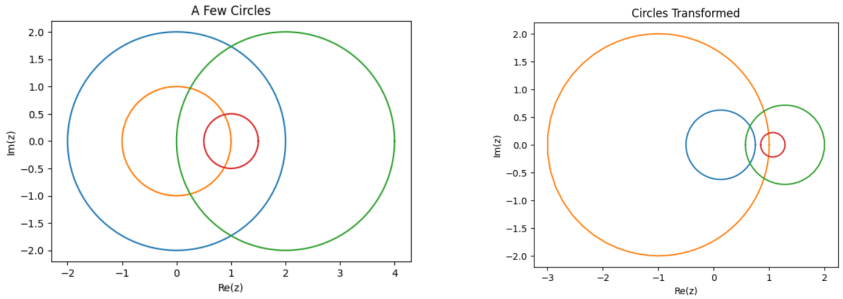

Pre-transformation Post-transformation

Figure 2: Möbius transform

transform using our theorem above.

$$\begin{aligned} f'(z) &= \frac{a(cz+d) - c(az+b)}{(cz+b)^2} \\ &= \frac{ad-bc}{(cz+d)^2} \end{aligned}$$

Note that with our initial condition $ad \neq bc$ and $z \neq -\frac{d}{c}$, this derivative is nonzero, so the map is conformal for all $z \neq -\frac{d}{c}$.

We will observe a few properties of this class of transforms in the example below.

Consider the transform $f(z) = \frac{z+4}{3z+2}$. We note that there is a singularity at $z = -\frac{2}{3}$. Consider the following circles drawn in the complex plane, then transformed by the Möbius transform in Figure 2.

Notice that around the singularity, $z = -\frac{2}{3}$, the transform appears to be inverted, but circles still preserve their shape. Circles that enclose the singularity are enlarged, and those that do not grow smaller. All circles tend to move away from the singularity.

Note that figures were produced in `Python` by defining circles and mapping them according to the transformation in `matplotlib`.

We can construct many different classes of conformal mappings, such as the one above with various desired properties. We will continue to explore certain classes of transformations in the applications section.

Furthermore, it is important to observe that Laplace's Equation is also satisfied in the conformally mapped plane, except at certain points, which are defined and understood by the following theorem:

Theorem 2. *If two simply-connected domains $\mathcal{D}$ and $\mathcal{D}'$ are related with a conformal mapping $f(x,y) = u(x,y) + iv(x,y)$, then the Laplacian $\nabla^2\phi(x,y)$ on $\mathcal{D}$ is related to the Laplacian $\nabla^2\psi(u,v)$ on $\mathcal{D}'$ by*

$$\nabla^2\psi(u,v) = |\nabla x(u,v)|^2 \nabla^2\phi(x,y) \tag{2}$$

[2]

Proof. Begin with ψ_{uu}:

$$\begin{aligned}\psi_{uu} &= \frac{\partial}{\partial u}\left(\phi_x \frac{\partial x}{\partial u} + \phi_y \frac{\partial y}{\partial u}\right) \\ &= \frac{\partial \phi_x}{\partial u}\frac{\partial x}{\partial u} + \phi_x \frac{\partial^2 x}{\partial u^2} + \frac{\partial \phi_y}{\partial u}\frac{\partial y}{\partial u} + \phi_y \frac{\partial^2 y}{\partial u^2} \\ &= \phi_{xx}\left(\frac{\partial x}{\partial u}\right)^2 + \phi_{yy}\left(\frac{\partial y}{\partial u}\right)^2 + 2\phi_{xy}\frac{\partial x}{\partial u}\frac{\partial y}{\partial u} + \phi_x \frac{\partial^2 x}{\partial u^2} + \phi_y \frac{\partial^2 y}{\partial u^2}\end{aligned}$$

Again, for ψ_{vv}

$$\psi_{vv} = \phi_{xx}\left(\frac{\partial x}{\partial v}\right)^2 + \phi_{yy}\left(\frac{\partial y}{\partial v}\right)^2 + 2\phi_{xy}\frac{\partial x}{\partial v}\frac{\partial y}{\partial v} + \phi_x \frac{\partial^2 x}{\partial v^2} + \phi_y \frac{\partial^2 y}{\partial v^2}$$

Then, we find

$$\begin{aligned}\psi_{uu} + \psi_{vv} &= \phi_{xx}\left(\left(\frac{\partial x}{\partial u}\right)^2 + \left(\frac{\partial x}{\partial v}\right)^2\right) + \phi_{yy}\left(\left(\frac{\partial y}{\partial u}\right)^2 + \left(\frac{\partial y}{\partial v}\right)^2\right) + 2\phi_{xy}\left(\frac{\partial x}{\partial u}\frac{\partial y}{\partial u} + \frac{\partial x}{\partial v}\frac{\partial y}{\partial v}\right) + \\ &\quad \phi_x\left(\frac{\partial^2 x}{\partial u^2} + \frac{\partial^2 x}{\partial v^2}\right) + \phi_y\left(\frac{\partial^2 y}{\partial u^2} + \frac{\partial^2 y}{\partial v^2}\right) \\ &= \phi_{xx}\left(\left(\frac{\partial x}{\partial u}\right)^2 + \left(\frac{\partial x}{\partial v}\right)^2\right) + \phi_{yy}\left(\left(\frac{\partial y}{\partial u}\right)^2 + \left(\frac{\partial y}{\partial v}\right)^2\right) + 2\phi_{xy}\left(\frac{\partial x}{\partial v}\frac{\partial x}{\partial u} - \frac{\partial x}{\partial v}\frac{\partial x}{\partial v}\right) \\ &= (\phi_{xx} + \phi_{yy})\left(\left(\frac{\partial x}{\partial u}\right)^2 + \left(\frac{\partial x}{\partial v}\right)^2\right) \\ &= (\phi_{xx} + \phi_{yy})|\nabla x(u,v)|^2\end{aligned}$$

Thus, $\nabla^2 \psi(u,v) = |\nabla x(u,v)|^2 \nabla^2 \phi(x,y)$ □

Ideal Fluid Flow

We will now explore the use of conformal maps to simplify the analysis of ideal fluids. Since functions transformed by a conformal map also satisfy Laplace's Equation (because of their analyticity), we can solve more complex ideal fluid problems by transforming flows from a known solution in a simpler domain, such as the upper-half plane (UHP) or the unit circle, into a flow in the original domain.

Suppose we wish to study the flow around an interior corner in the first quadrant $Q = \{z \mid x > 0, y > 0\} \subset \mathbb{C}$. We use the conformal map $w = z^2$ to transform Q into the UHP. We then solve for the uniform potential flow in the w-plane:

$$\hat{\Omega}(w) = Aw$$

Finally, we substitute to obtain our solution in the z-plane:

$$\Omega(z) = Az^2 = A(x+iy)^2 = A(x^2 - y^2 + 2ixy) \implies \Psi(x,y) = 2Axy$$

which gives the expected result shown on the left of Figure 3 [3]

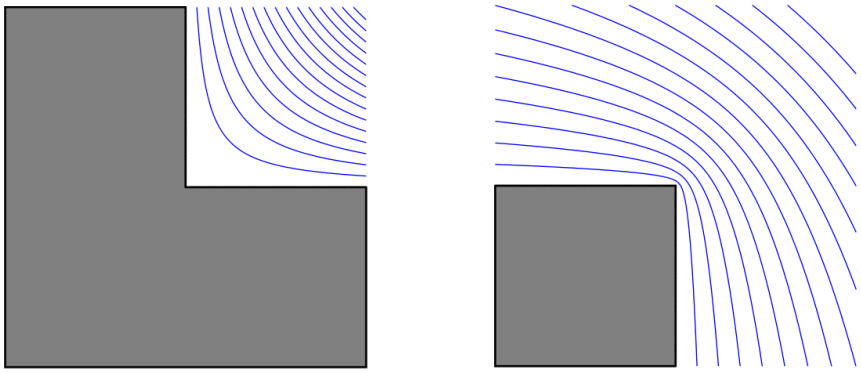

$\Omega(z) = z^2$ $\Omega(z) = (iz)^{2/3}$

Figure 3: Streamlines of resulting corner flows

Similarly, we can find the flow around an exterior corner, for example one occupying the third quadrant. By using the map $w = (iz)^{2/3}$ we can transform $Q = \mathbb{C} \setminus \{z \mid x < 0, y < 0\}$ to the UHP. As before, have uniform flow in the w-plane

$$\hat{\Omega}(w) = Aw$$

and we substitute z back in to obtain our solution in the original z-plane:

$$\Omega(z) = A(iz)^{2/3} \implies \Psi(x,y) = \sqrt{x^2+y^2}^{2/3} \sin\left(\frac{2}{3}\left(\arctan(y/x) + \pi/2\right)\right)$$

the streamlines of which are shown on the right of Figure 3.

Joukowski Transform

We can extend these ideas of transformations to study flow around more complex solid bodies. We now introduce the Joukowski Transform, given by

$$w = \frac{1}{2}\left(z + \frac{1}{z}\right)$$

Using the form $z = re^{i\theta}$, we can see that

$$\begin{aligned} w &= \frac{1}{2}\left(re^{i\theta} + \frac{1}{re^{i\theta}}\right) \\ &= \frac{1}{2}\left(\cos\theta\left(r + \frac{1}{r}\right) + i\sin\theta\left(r - \frac{1}{r}\right)\right) \end{aligned}$$

It can be seen that w will collapse the unit circle ($r = 1$) down to the segment $[-1, 1]$ on the real line. Larger circles will be mapped to ellipses with foci at $z = \pm 1$; these can be seen in Figure 4. We can use this transformation to find the flow around a cylinder of unit radius centered at the origin. w will map the cylinder in the z-plane onto a flat plate in the w-plane; the flat plate will not affect the flow of fluid over it, leading again to a uniform flow in the w-plane:

$$\hat{\Omega}(w) = Aw$$

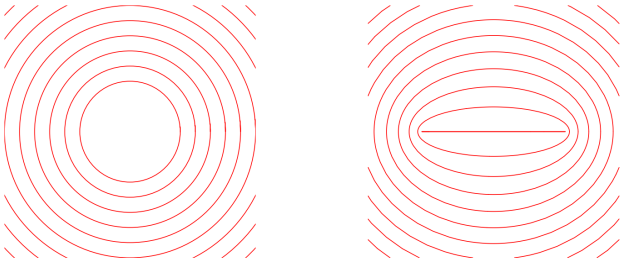

Figure 4: Joukowski Transform applied to concentric circles [4]

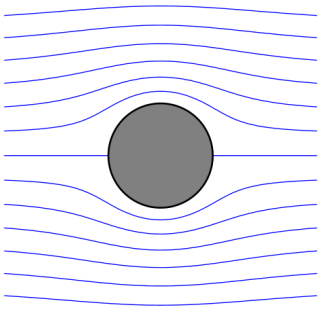

Figure 5: Flow around the unit cylinder

Substituting back, we get the flow in the z-plane:

$$\Omega(z) = \frac{A}{2}\left(z + \frac{1}{z}\right) \implies \Phi(x,y) = \frac{Ay}{2} - \frac{Ay}{2(x^2+y^2)}$$

The streamlines can be found in Figure 5. We observe that this is the same result as uniform flow superimposed with a dipole.

The Joukowski transformation provides interesting results when applied to circles not centered at the origin. Let $z = z_0 + re^{i\theta}$, then

$$\begin{aligned} w &= (z_0 + re^{i\theta}) + \frac{1}{(z_0 + re^{i\theta})} \\ &= z_0 + re^{i\theta} + e^{-i\theta}\frac{1}{z_0 e^{-i\theta} + r} \end{aligned}$$

Now consider what the transform result will be. For small values of θ, the function behaves like $w \approx z_0 + r + \frac{1}{z_0+r}$. For values near $\theta = \frac{\pi}{2}$, it behaves like $w \approx z_0 + ir + \frac{i}{-iz_0+r}$. Near $\theta = \pi$, $w \approx z_0 - r - \frac{1}{r-z_0}$. Thus, we expect to see cusp behavior on the tail end of the transform, but more elliptical behavior on the alternate end.

Some examples of configurations can be seen in Figure 6. The shape can be made remarkably close to that of an airfoil and the transformation was historically used to understand flows around airfoils via the same fluid analysis as applied to the cylinder.

To analyze the fluid flowing around this, we construct a uniform flow with an angle of 20°and model the result with the airfoil with parameters $z_0 = -0.15 + .34i, r = 1.4$, as seen in Figure 7. Figures were constructed using the Python module `pflow` [5] and transforming the uniform flow

$z_0 = 0.6,\ r = 1.2$ $z_0 = -1.85 + 0.5i,\ r = 1.3$ $z_0 = -0.15 + 0.34i,\ r = 1.4$

Figure 6: Joukowski Transform applied to unit disk

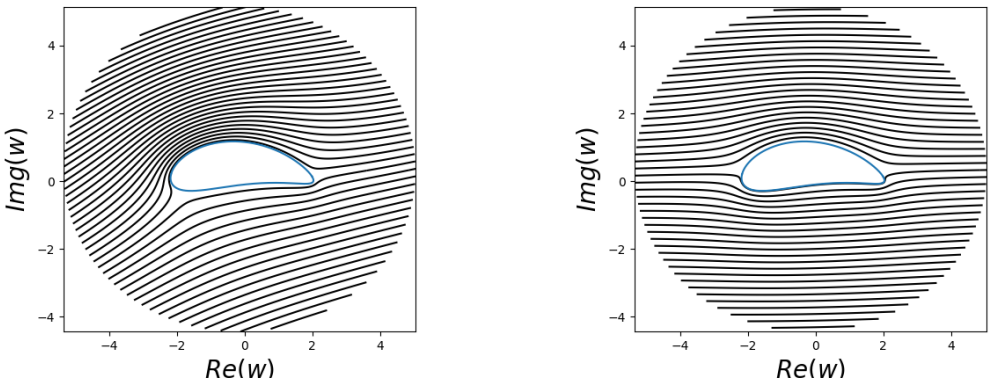

(a) Uniform flow at 20° (b) Uniform flow at 5°

Figure 7: Joukowski Streamlines

with the Joukowski.
We observe the expected flow around an airfoil, and further, we can continue this analysis to compare different airfoils, simulate the lift and drag, and model varying angles of flow.

Conclusion and Future Directions

Conformal mapping utilizes many of the helpful properties of analytic functions to enable mathematicians to represent and analyze physical scenarios. We begin by showing important properties of conformal mappings and introduce several examples with great utility. We then show that Laplace's Equation is preserved through conformal mapping, and consequently we can use this result to study more complicated flows, and extension of the standard use of complex variables to ideal fluid flow. We can extend the results of fluid flow to other transforms, and here, we study the Joukowski Transform, which maps circles centered on the origin to ellipses and circles centered off the origin to curved shapes, many of which can be constructed to resemble airfoils. Then, we can apply the ideas of fluid flow to study how the airfoil behaves with only a simple transform, as opposed to other computationally complex methods.

One major limitation with this analysis is the assumption of ideal fluid flow. While this is a reasonable assumption for lower speeds, it fails to hold up to real-world speeds. Specifically, the incompressibility assumption fails to hold for liquids and gases traveling at speeds greater than Mach 0.3 [6]. In fact, here, there are many other factors that play a role, including heat from friction, compressibility effects, and chemical decomposition of the fluid, and ultimately, these factors dominate.

Future work could involve other classes of conformal maps, since many of these have useful applications. For example, spherical geometry can be greatly simplified through the Möbius transform introduced above. Such work could involve extensions of the Joukowski to further analyze the tail end under less ideal conditions than assumed above through more complicated conformal maps, for example, through a Kármán–Trefftz transform. Further, similar physical situations could be modelled numerically and compared to the ideal case in order to understand where the incompressibility and irrotational assumptions contribute to error most significantly. Finally, methods to analyze lift given Joukowski transforms could be employed to again bring complex analysis closer to the real-world result.

References

[1] MathWorks, "Exploring a conformal mapping." https://www.mathworks.com/help/images/exploring-a-conformal-mapping.html. [Accessed 20-04-2024].

[2] W. Lan, "Conformal mapping and its application to laplace's equation," 2019.

[3] Caltech, "Conformal mapping." http://brennen.caltech.edu/fluidbook/basicfluiddynamics/potentialflow/complexvariables/conformalmapping.pdf, 2006. [Accessed 28-04-2024].

[4] P. J. Olver, *Complex Analysis and Conformal Mapping*. University of Minnesota, 2024.

[5] B. Kamath, "Joukowsky-airfoil." https://github.com/bharath-kamath705/Joukowsky-Airfoil/blob/master/joukowski_airfoil.py, 2019. [Accessed 28-04-2024].

[6] E. White, "Insights from an aerospace engineer about ideal fluid flow." Interview, April 27, 2024.

[7] M. Cavarga, "Modeling of fluid flow past solid objects via complex analysis," 2019.